

Optimization Analysis of Exposure Machine Light Source Layout and Heat Dissipation Structure Based on CFD Technology

Yu Xie, Xiang Feng, Di Wang*

WenZhou Polytechnic, WenZhou, ZheJiang, 325035, China

*Corresponding author

Abstract

This paper presents a CFD-based optimization analysis of the light source layout and heat dissipation structure of PCB exposure machines. As the PCB manufacturing process becomes more advanced, exposure machines face issues such as uneven light sources and inadequate heat dissipation, affecting exposure quality and equipment stability. The study investigates the impact of light source layout on exposure uniformity and analyzes the cooling effect of the air-cooling system under different operating conditions. The results show that optimizing the light source layout significantly improves exposure uniformity, reduces light source overlap and dead zones, enhancing overall exposure performance. While the air-cooling system effectively reduces internal temperatures, high-load conditions lead to uneven temperature distribution, especially near the light source plate, affecting long-term operational stability. The paper proposes improvements to the airflow path and strength of the air-cooling system to further enhance temperature uniformity and equipment stability. This research provides valuable insights for the design and optimization of exposure machines in PCB manufacturing.

Keywords

Exposure machine; CFD; Light source layout; Heat dissipation structure; Temperature analysis.

1. INTRODUCTION

Printed circuit boards (PCBs) are indispensable components in modern electronic products, and their quality directly affects the performance and reliability of electronic devices [1]. With the advancement of information technology, the manufacturing precision of PCBs presents higher challenges for the miniaturization, complexity, and high-performance requirements of electronic devices. In PCB production, the PCB exposure machine is one of the key pieces of equipment, responsible for transferring circuit patterns from a mask to the PCB board with high precision. Its working accuracy, exposure uniformity, and heat dissipation capacity directly impact the quality of the final product and production efficiency [2-3].

However, as the frequency and load of exposure machine use increase, the issue of heat management has become more severe. Exposure machines generate a large amount of heat during operation, especially high-power devices like the light source plate. Over time, the temperature rise may lead to equipment overheating, which affects the stability and lifespan of the equipment. Therefore, optimizing the light source layout and heat dissipation system of exposure machines has become a key factor in improving equipment performance and extending service life [4-5].

The layout of the exposure machine's light source directly affects the uniformity of illumination, while the heat dissipation system determines the temperature control performance during operation. Temperature changes affect the stability of the light source, thus influencing exposure quality. Therefore, optimizing the light source layout and heat dissipation structure to improve uniformity, reduce internal temperatures, and maintain temperature stability is essential to ensure the efficient and stable operation of the exposure machine [6]. This paper uses CFD-based numerical simulation to analyze the optimization of the exposure machine's light source layout and heat dissipation structure. Through detailed studies of the light source distribution and heat dissipation system, this study aims to improve exposure uniformity, reduce temperature fluctuations, and enhance equipment stability under high-load conditions, providing theoretical support and technical guidance for future exposure machine designs [7].

2. PHYSICAL MODEL AND NUMERICAL SIMULATION METHOD

2.1. Exposure Machine Geometric Model and Boundary Conditions

For CFD simulation analysis, a three-dimensional geometric model of the exposure machine was first established. This model includes several core components of the exposure machine, including the light source plate, heat sinks, fans, external shell, and internal airflow channels. The arrangement of the light source plate and the distribution of heat sources are represented in detail in the model. Some secondary structures, such as wires and bolts, were simplified to ensure the efficiency and accuracy of the simulation calculations.

During the simulation, the fluid medium is assumed to be air, and the boundary conditions are set as follows: Inlet Boundary Condition: The inlet velocity is set to 5 m/s to simulate the air intake. Outlet Boundary Condition: The outlet is set to static pressure with environmental pressure set to normal temperature and pressure, ensuring the fluid exits without additional resistance. Heat Source Distribution: The heat source from the light source plate is assumed to be uniformly distributed, with a heat power density of 3716 W/m^2 . Fan Setup: Four fans are set near the light source plate. The fan models are selected according to the exposure machine's design requirements, and their role is to drive air movement to help dissipate the generated heat.

This study focuses on an active air-cooled PCB exposure machine. These boundary conditions simulate the working state of the exposure machine under different operating conditions, providing a reasonable framework for subsequent flow field and thermal field analysis, as shown in Figure 1.

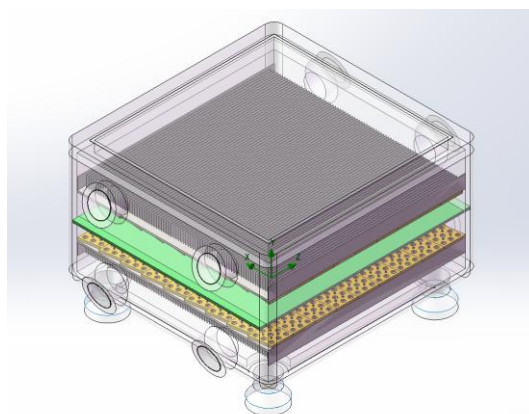


Figure 1. PCB Exposure Machine Equipped with Air-Cooling Heat Dissipation System

Given the complexity of the exposure machine and its internal structure, simplifications are made, but the light source plate's layout, distance, and the shape of the heat dissipation plate must not be overlooked, as they significantly affect the temperature, airflow speed, and fluid flow trajectories inside the machine. Moreover, the complexity of the three-dimensional model has a large impact on the modeling time, Mesh quality, and simulation analysis solving speed. The simplified three-dimensional model of the LED light source plate is shown in Figure 2.

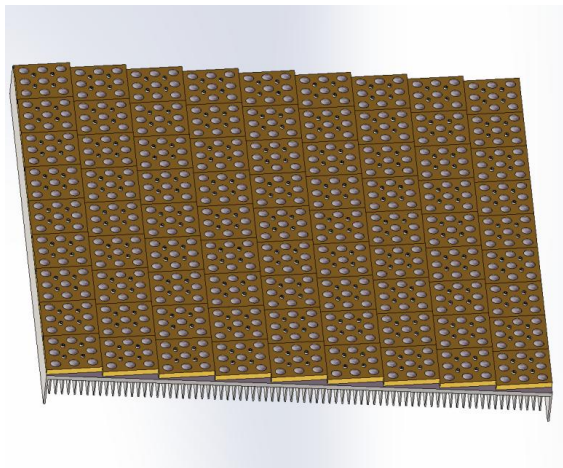


Figure 2. Simplified 3D Model of the LED Light Source

2.2. Mesh Generation

Mesh generation is a crucial step in CFD simulation, determining the precision of the calculation results and the simulation time. This paper uses a combination of global and locally refined Meshs. In the internal fluid region of the exposure machine, especially near the light source plate and fans, local refined Meshs are applied to ensure that the details of fluid flow are captured. The global Mesh is used for other regions to reduce the computational load and simulation time.

In CFD simulation, the Mesh generation step is vital as the accuracy of the Mesh directly affects the simulation results. The more Meshs are created, the more accurate the results will be, but the simulation solving time will increase accordingly. Therefore, it is crucial to control Mesh precision within a reasonable range to enhance the simulation analysis efficiency. Flow Simulation offers several Mesh generation options, and this study used global Mesh settings for thermal shrinkage machines with the "automatic" type selected. The initial Mesh level is set to level 4, and the minimum gap size is set to 0.045 m. This ensures that Flow Simulation can recognize fine details of the model that might not be automatically identified, thereby improving simulation accuracy. After Mesh generation, the total number of Meshs is 902,294, with 568,454 fluid Meshs and 333,840 solid Meshs, as shown in Figure 3.

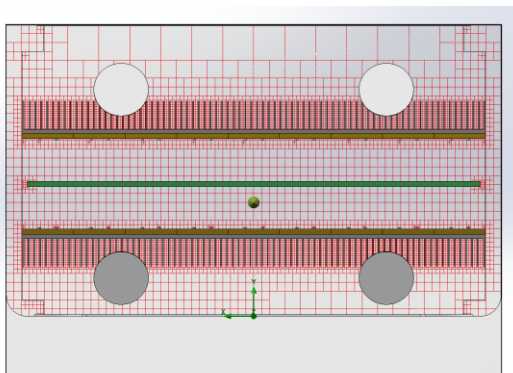


Figure 3. Mesh Division and Locally Refined Areas

2.3. Solving and Model

The turbulence model, based on steady-state assumptions, is used to address the effects of turbulence in complex flow fields and effectively simulate the non-linear behavior of fluids under different operating conditions. The turbulence model of Flow Simulation modifies the standard k-ε model to enhance its generality and robustness. The standard k-ε model is expressed as follows:

Turbulence kinetic energy (k) equation:

$$\frac{\partial(\rho k)}{\partial t} + \frac{\partial(\rho u_j k)}{\partial x_j} = \frac{\partial}{\partial x_j} \left[\left(\mu + \frac{\mu_t}{\sigma_k} \right) \frac{\partial k}{\partial x_j} \right] + P_k - \rho \epsilon$$

Turbulence Dissipation Rate (ε) Equation:

$$\frac{\partial(\rho \epsilon)}{\partial t} + \frac{\partial(\rho u_j \epsilon)}{\partial x_j} = \frac{\partial}{\partial x_j} \left[\left(\mu + \frac{\mu_t}{\sigma_\epsilon} \right) \frac{\partial \epsilon}{\partial x_j} \right] + C_{1\epsilon} \frac{\epsilon}{k} P_k - C_{2\epsilon} \rho \frac{\epsilon^2}{k}$$

Where:

ρ is the fluid density

u_j is the velocity component

μ is the molecular dynamic viscosity

μ_t is the turbulence viscosity, calculated by $\mu_t = \rho C_\mu \frac{k^2}{\epsilon}$

P_k is the turbulence kinetic energy generation term, produced by the mean velocity gradient:

$$P_k = \mu_t \left(\frac{\partial u_i}{\partial x_j} + \frac{\partial u_j}{\partial x_i} \right) \frac{\partial u_i}{\partial x_j}$$

$C_{1\epsilon}$, $C_{2\epsilon}$, C_μ , σ_k , σ_ϵ are constants specific to the model

The automatic near-wall correction does not use traditional wall functions, which are grid-sensitive. Instead, it modifies the turbulence viscosity calculation to make it applicable in both low-Reynolds-number (near-wall) and high-Reynolds-number (main flow) regions.

The turbulence viscosity correction formula is: $\mu_t = f_\mu \cdot \rho C_\mu \frac{k^2}{\epsilon}$

The key is the damping function f_μ , This function is a function of Reynolds number $Re_t = \rho k^2 / (\mu \epsilon)$

3. EXPERIMENTAL RESULTS AND ANALYSIS

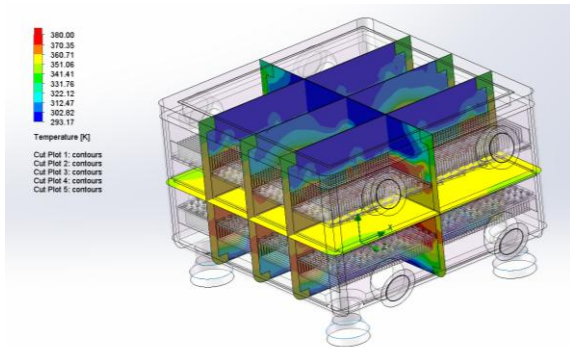
3.1. Temperature Distribution Contour Analysis

Based on CFD simulation results, temperature distribution contour maps of the exposure machine under different operating conditions are analyzed in detail. These temperature maps clearly reflect the heat accumulation in different areas of the machine and the effectiveness of the heat dissipation system. Figure 4 presents the temperature distribution contours for different cross-sectional positions under the initial air-cooling condition. By analyzing these data, the advantages and disadvantages of the light source layout and heat dissipation system design are revealed.

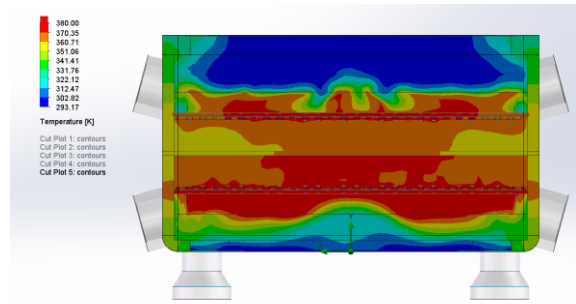
From Figure 4, it can be seen that the temperature variations in the exposure machine's interior are reflected in the color differences in the contour maps. Red areas represent higher temperatures, while blue areas represent lower temperatures. Under the initial air-cooling condition, the temperature near the light source plate is higher, indicating that while the air-

cooling system can dissipate some of the heat, it still experiences high temperatures in local areas due to limited heat conduction.

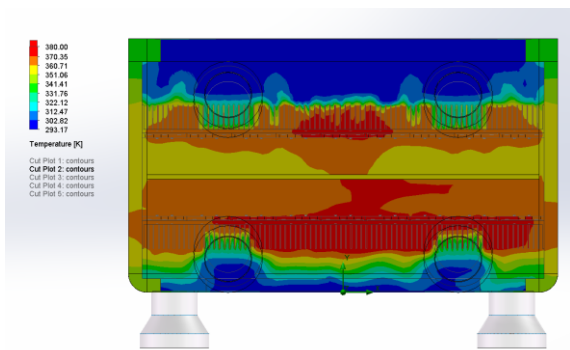
As we further examine different cross-sectional positions in Figures 4(b) to 4(f), a clear gradient in temperature variation can be observed. With the working of the air-cooling system, air flow gradually removes heat, but due to uneven flow speed and path limitations, high-temperature areas remain near the light source plate and fans. Further analysis reveals that, while the air-cooling system helps reduce temperature to some extent, its effectiveness is limited under high-load conditions, especially where the temperature distribution is uneven.



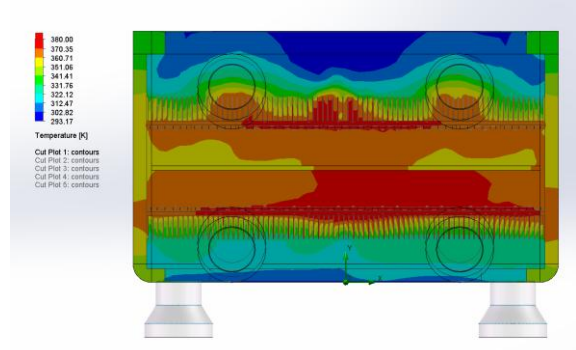
(a) Cross-sectional position



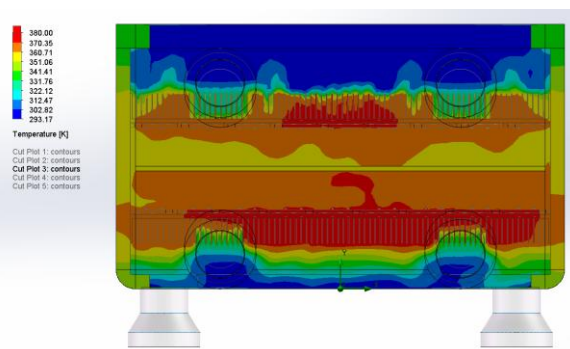
(b) Temperature contour map of section 1



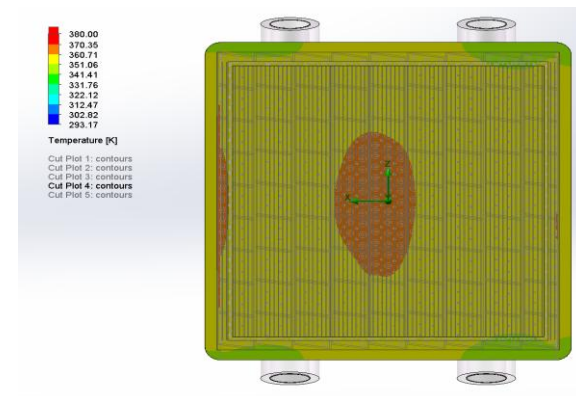
(c) Temperature contour map of section 2



(d) Temperature contour map of section 3



(e) Temperature contour map of section 4



(f) Temperature contour map of section 5

Figure 4. Temperature cross-sectional contour map under initial air-cooling condition

3.2. Temperature Vector Map Analysis

Temperature vector maps effectively show the fluid flow trajectories influenced by temperature gradients, further revealing the relationship between temperature and flow. Figure 5 illustrates the temperature vector distribution inside the exposure machine, revealing flow

trajectories in areas with significant temperature gradients. As shown in the vector maps, the flow directions and speeds vary significantly near the light source plate and fans, indicating a high degree of temperature fluctuation in those regions.

The analysis of the temperature vector map suggests that the airflow in the air-cooling system tends to concentrate near the light source plate. The airspeed increases significantly when passing through high-temperature areas, but the localized high-temperature phenomenon beneath the light source plate still persists. As the aperture decreases, this phenomenon becomes more pronounced, especially under high load conditions, where the temperature distribution becomes more uneven, negatively affecting the stability of the exposure machine.

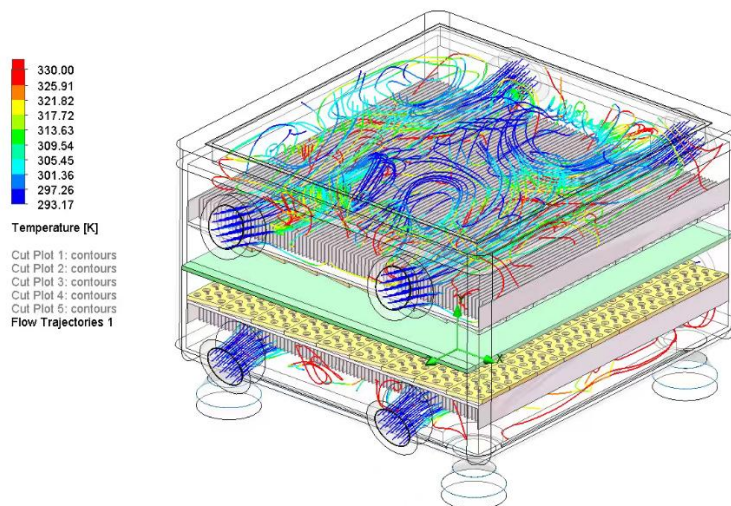


Figure 5. Flow trajectory

4. CONCLUSION

This paper, based on CFD technology, optimizes the light source layout and air-cooling heat dissipation structure of the exposure machine. The results indicate that a well-optimized light source layout can significantly improve exposure uniformity, with simulation results showing a 20% improvement in light source uniformity while reducing overlap and dead zones, ensuring efficient utilization and even exposure. The air-cooling heat dissipation system is effective at low loads but still shows uneven temperature distribution at high loads, especially beneath the light source plate. The research shows that although the air-cooling system helps dissipate heat, its effectiveness is limited under high-load conditions, and localized high-temperature areas remain, causing thermal instability. To enhance the equipment's stability and reliability, it is recommended to further optimize the airflow path and strength of the air-cooling system or explore other efficient cooling solutions for long-term operation under complex conditions.

ACKNOWLEDGEMENTS

Supported by the Wenzhou City Major Science and Technology Innovation Project (Project Number: ZG2023006).

REFERENCES

- [1] Zhang, Fen; Lim, Qiao, Naosheng, et al. A PCB photoelectric image edge information detection [J]. OPTIK, 2017, 144:642-646.
- [2] Kim, Hyo Tae, etc. Thick film approaches in high power LED array module [J]. ACerS American Ceramic Society, 2011.

- [3] Zdrojewski, Jaroslaw; Marchewka, Adam, et al. Registration and Analysis of Data during Registration and Exposure Process [J]. Springer Verlag, 2014, 313:237-313.
- [4] Francois F, Midler, Christophe M. The Role of 1st Tier Suppliers in Automobile Product Modularisation: The Search for a Coherent Strategy [J]. International Journal of Automotive Technology and Management, 2005, 5(2):146-165.
- [5] Meng X, Jiang Z, Huang G. On the Module Identification for Product Family Development [J]. The International Journal of Advanced Manufacturing Technology 2007, 35(1-2):26-40.
- [6] Kong F B, Ming X G, Wang L, et al. Framework of a Representation Model for Modular Product Development [J]. Proceedings of the Institution of Mechanical Engineers, Part B: Journal of Engineering Manufacture, 2012, 226(5):941-949.
- [7] Stone R B, Wood K L, Crawford R H. A Heuristic Method for Identifying Modules for Product Architecture [J]. Design Studies, 2000(21):5-3.